Research Article | Vol. 30, No. 23 / 7 Nov 2022 / Optics Express 41157
Optics EXPRESS

H_∞ filter-based dynamic joint carrier frequency offset and linear phase noise tracking for CO-OFDM systems

SHUAI LIU,[1] XINWEI DU,[1,2,*] AND CHANGYUAN YU[3]

[1]Faculty of Science and Technology, BNU-HKBU United International College, Zhuhai 519087, China
[2]Guangdong Provincial Key Laboratory of Interdisciplinary Research and Application for Data Science, BNU-HKBU United International College, Zhuhai 519087, China
[3]Department of Electronic and Information Engineering, The Hong Kong Polytechnic University, Hung Hom, Hong Kong
*xinweidu@uic.edu.cn

Abstract: In this paper, a robust, dynamic and joint carrier frequency offset (CFO) and linear phase noise (LPN) tracking algorithm is proposed by utilizing the H_∞ filter for CO-OFDM systems. The dynamic tracking is implemented by Bayesian filtering which time-recursively updates the posterior state estimates based on the prior state information and calculated gain. To improve the robustness of the dynamic tracking process against the uncertainty of the noise terms, we adopt the H_∞ filter, which designs a min-max optimization problem with a performance bound-defined constraint. The H_∞ filter obtains the state estimates by limiting the worst-case estimation error, which guarantees its robustness to the system uncertain noise terms and external disturbances. After the joint estimation of CFO and LPN, we then propose a decision-feedback algorithm to achieve accurate signal detection. The accuracy and robustness of the proposed algorithm are verified in an 88.9 Gb/s 16-QAM CO-OFDM system, by comparing with the conventional extended Kalman filter (EKF) and Gaussian particle filter (GPF). Simulation results show that the MSEs of CFO and LPN by H_∞ filter can reach the Cramér-Rao Lower Bounds (CRLBs) as well as the Bayesian CRLB (BCRLB), and possesses excellent noise and chromatic dispersion (CD) tolerance.

1. Introduction

Coherent optical orthogonal frequency-division multiplexing (CO-OFDM) is a multi-carrier modulation (MCM) technique which has attracted much research attention in optical communication systems due to its high spectral efficiency and robustness to chromatic dispersion (CD) and polarization mode dispersion (PMD) [1]. However, the CO-OFDM is sensitive to the carrier frequency offset (CFO) and linear phase noise (LPN), which can introduce inter-carrier interference (ICI) to the system, thus degrade its bit error rate (BER) performance.

Various approaches have been proposed for the estimation and compensation of CFO and LPN. From the flexibility of the algorithms, these estimation approaches can be divided into two types, static estimation and dynamic estimation. Most of the static approaches focus on the offline estimation of CFO and LPN, either individually or jointly. In static estimation, the variation of dynamic parameters like phase noise are assumed to be slow, so that they can be treated as constants within a certain length. A constant modulus-based CFO estimation algorithm is proposed in [2]. The proposed method achieves stable and efficient estimation with low complexity which is robust against fiber dispersion. However, the cost function in [2] is approximated to a cosine function and the CFO estimate is obtained by given three test values, which leads to the estimation accuracy being dependent on the discrete Fourier transform (DFT) size and the number of transmitted OFDM symbols. In [3], a joint timing offset (TO), CFO and

#468086 https://doi.org/10.1364/OE.468086
Journal © 2022 Received 23 Jun 2022; revised 9 Oct 2022; accepted 10 Oct 2022; published 25 Oct 2022

Optics EXPRESS

phase estimation approach is proposed by matched filtering. The estimation performance can reach the Cramér-Rao Lower Bound (CRLB) with low implementation complexity. However, the phase noise here is assumed to be a constant phase, which is estimated by using the first OFDM symbol only, thus this method lacks the phase noise estimation for the entire received signal. In [4], a joint maximum *a posterior* probability (MAP) estimation of channel states and the frequency offset was introduced, which can achieve much better performance than the maximum likelihood (ML) estimation. However, this method requires to utilize 20 OFDM pilot symbols to ensure the estimation accuracy and it is actually a sequential algorithm, which reduces the effective transmission bit rate and efficiency. A pilot-aided (PA) phase estimation approach is proposed in [5]. The estimation of the common phase error (CPE) on each OFDM symbol is obtained by taking the phase average of the pilot subcarriers. This method is straightforward and simple, but the phase estimation performance is highly dependent on the number of pilot subcarriers. In general, static approaches ensure the estimation performance by utilizing the training or pilot symbols which sacrifice the effective transmission bit rate. In addition, the offline estimation manner does not satisfy the requirement of real-time signal processing in practical optical transmission systems. Therefore, dynamic algorithms are in need to provide more flexible estimations while at the same time guaranteeing the accuracy.

The Bayesian filter is one of the most popular approaches for dynamic state tracking. Among the Bayesian filters, the particle filter (PF) is suitable for nonlinear state estimation with non-Gaussian noises. However, the common disadvantage of PFs is the degeneracy phenomenon of particles, which can be solved by using resampling [6]. However, in the conventional sequential importance resampling (SIR) PF [7,8], the particle impoverishment (PI) problem causes that the particles with high weights being duplicated statistically for many times, which may cause severe estimation performance degradation especially when the particle number is small. In [9], a Gaussian particle filter (GPF) approach is proposed where the resampling process is not needed. This approach avoids the PI problem and outperforms other traditional PFs. However, the performance of a PF is highly dependent on the number of particles, and the increase of the particle number will lead to an increase on the computational complexity of the algorithm. The extended Kalman filter (EKF) is widely used for the dynamic state estimation due to its low complexity and fast convergence. The EKF performs the first-order Taylor expansion to linearize the nonlinear state and observation functions. It then apply the linear KF to deal with the state estimations. A phase noise tracking method is proposed in [10], based on the adaptive EKF, which is moderately less complicated and more flexible. The authors in [11] also utilized the EKF to jointly estimate the CFO and the carrier phase noise. However, EKF has two main disadvantages. Firstly, since the EKF performs the first-order Taylor expansion on the nonlinear functions, the forecast value calculated by the approximated functions may differ from the actual value, which will affect the state estimation accuracy. Secondly, EKF requires the noise distribution to be Gaussian and the noise covariance matrix to be known. However, in real optical transmission systems, the noise statistics are usually unknown. Therefore, a robust, dynamic and joint CFO and LPN tracking algorithm is desired to deal with the uncertain noise statistics and disturbances.

In this paper, we propose an H_∞ filter-based approach to dynamically and jointly track the CFO and LPN, then a decision-feedback signal detection method is derived to ensure the BER performance. Firstly, by solving the min-max optimization problem with a given threshold, we can recursively update the prior state information and the H_∞ gain, thereby obtaining the posterior state estimate. The min-max optimization problem protects the tracking performance from severe noise disturbances, which illustrates the robustness of the proposed H_∞ filter algorithm. Secondly, after compensating for the CFO in the received signal, we apply a decision-feedback method to accurately detect the bit sequence. The unknown transmitted OFDM symbol is firstly determined by compensating the coarse LPN estimate based on the averaged phase estimates on the previous OFDM symbol. A fine LPN estimation is conducted by utilizing the H_∞ filter according to

Optics EXPRESS

the newly determined OFDM transmitted symbol. Thirdly, the CRLBs and Bayesian CRLB (BCRLB) are derived to evaluate and verify the state estimation performance of the proposed H_∞ filter. Finally, comparing with conventional Bayesian filters such as EKF and GPF in [9,11], as well as the classical Schmidl's method in [12], simulation results demonstrate that the proposed H_∞ filter can obtain the MSEs of CFO and LPN converging to the CRLBs and BCRLB even in the appearance of 20 dB external noise disturbance and residual CD.

2. Signal model

The n-th received CO-OFDM time-domain signal $r(n)$ can be expressed as:

$$r(n) = s(n-\tau) \otimes h(n) e^{j[\frac{2\pi\epsilon n}{N} + \theta(n)]} + w(n),\ n = 0, 1, \ldots, N-1 \tag{1}$$

where $s(n)$ is the n-th transmitted OFDM sample and N is the size of discrete Fourier transform (DFT). Term τ is the TO and $h(n)$ is the channel impulse response (CIR). $\otimes$ is the convolution operator and $w(n)$ is the complex additive white Gaussian noise (AWGN) with mean 0 and variance σ_w^2. Term ϵ is the CFO normalized by the OFDM subcarrier spacing, which can be divided into an integral part and a fractional part. $\theta(n)$ is the LPN which is commonly modelled as a Wiener process:

$$\theta(n) = \theta(n-1) + \nu(n) \tag{2}$$

where $\nu(n)$ is a Gaussian random variable with mean 0 and variance σ_ν^2. We have $\sigma_\nu^2 = 2\pi\Delta\nu t$, where $\Delta\nu$ is the combined laser linewidth (CLW) and t is the OFDM sample time interval.

The dynamic joint tracking and estimation of CFO and LPN is implemented under the assumptions that the channel dispersion and fiber nonlinearities have been totally compensated and the TO is removed by existing algorithms. Thus the simplified signal model can be expressed as:

$$r(n) = s(n) e^{j[\frac{2\pi\epsilon n}{N} + \theta(n)]} + w(n). \tag{3}$$

In the next section, we will rewrite Eq. (3) as the state space model (SSM) and deal with the parameter tracking problem by using the vector format.

3. H_∞ filter-based joint CFO and LPN tracking

3.1. State space model

In the CO-OFDM system, the state vector at time n is expressed as $\mathbf{z}_n = (\epsilon_n, \theta_n)^T$, which is composed of the parameters to be estimated, i.e., CFO and LPN. Here, since the CFO is assumed to be a constant, the corresponding state noise variance is 0. The state noise vector can be written as $\mathbf{v}_n = (0, \nu_n)^T$ and its covariance matrix is $Q_n = \begin{bmatrix} 0 & 0 \\ 0 & \sigma_\nu^2 \end{bmatrix}$. According to Eq. (3), the SSM can be expressed as:

$$\mathbf{z}_n = \begin{pmatrix} \epsilon_n \\ \theta_n \end{pmatrix} = f_{n-1}(\mathbf{z}_{n-1}, \mathbf{v}_n) = \begin{pmatrix} \epsilon_{n-1} \\ \theta_{n-1} \end{pmatrix} + \mathbf{v}_n \tag{4}$$

$$r_n = h_n(\mathbf{z}_n, w_n) = s_n e^{j[\frac{2\pi\epsilon_n n}{N} + \theta_n]} + w_n \tag{5}$$

where Eq. (4) is the state function while Eq. (5) is the observation function.

Optics EXPRESS

3.2. H_∞ filtering

In the state-space model, there are two noise terms, v_n and w_n, whose variances are σ_v^2 and σ_w^2, respectively. If the noise is Gaussian, EKF can derive the estimate with minimum mean squared error (MMSE). However, in practical transmission systems, the noise distribution is uncertain or even unknown. With the noise uncertainty, a robust estimator is in need. To solve this key problem, we propose to utilize the H_∞ filter to achieve the joint CFO and LPN estimation in a dynamic manner, which does not make any assumptions about the noise distribution and aims to minimize the worst-case estimation error.

In H_∞ filter-based estimation algorithm, we introduce a threshold, $\frac{1}{\lambda}$, which guarantees the robustness of the estimator. Since the direct minimization of the estimation error is not tractable, a performance bound is applied for finding an estimation strategy that satisfies the threshold. The optimization problem is defined as:

$$\min_{\hat{\mathbf{z}}_n} \max_{v_n, w_n, \mathbf{z}_0} \quad J = \frac{\sum_{n=0}^{N-1} ||\mathbf{z}_n - \hat{\mathbf{z}}_n||^2}{||\mathbf{z}_0 - \hat{\mathbf{z}}_0||^2_{P_0^{-1}} + \sum_{n=0}^{N-1} \left(||\mathbf{v}_n||^2_{Q_n^{-1}} + ||w_n||^2_{R_n^{-1}} \right)} \qquad s.t. \;\; J < \frac{1}{\lambda} \tag{6}$$

where P_0 is the initial estimation error covariance matrix, Q_n is the covariance matrix for state noise vector $\mathbf{v}_n$ and R_n is the variance of w_n, i.e., σ_w^2. Besides, P_0 and R_n are symmetric, positive definite matrices. The value of J can be made less than $\frac{1}{\lambda}$ while the value of λ is determined by user. Thus the estimation process can be treated as a min-max optimization problem where the objective is to find an estimate $\hat{\mathbf{z}}_n$ to get the minimum value of J meanwhile the following constraint must hold to ensure that the H_∞ gain can be calculated:

$$P_n^{-1} - \lambda I + H_n^H R_n^{-1} H_n > 0 \tag{7}$$

for $n = 1, \ldots, N-1$, where $(\cdot)^H$ is conjugate transpose operation. After calculation, we can obtain the range of λ

$$0 < \lambda < \lambda_{max} \tag{8}$$

where $\lambda_{max} = \max \left\{ \frac{1}{2}\text{tr}(A_n) - \sqrt{\frac{1}{4}\text{tr}(A_n)^2 - |A_n|} \right\}$ and we have $A_n = P_n^{-1} + H_n^H R_n^{-1} H_n$, $\text{tr}(\cdot)$ is the trace of a matrix and $|\cdot|$ is the determinant of a matrix. A special case is that when $\lambda = 0$, the H_∞ filter will become EKF. This is because the EKF merely minimizes the mean squared error, but has no limitations of severely noisy environments, which is equivalent to set the performance bound of H_∞ filter to infinity.

The algorithm for joint CFO and LPN tracking based on the H_∞ filter is shown in Algorithm 1. In the algorithm, term F_{n-1} represents the partial derivative matrix of f_{n-1} with respect to $\mathbf{z}$ and $\mathbf{v}$ at $\mathbf{z}_{n-1}^+$. Term H_n stands for the partial derivative vector of h_{n-1} with respect to $\mathbf{z}$ at $\mathbf{z}_n^-$. At the initial stage, we treat that the CFO and LPN are independent with each other, and both are uniformly distributed, i.e., $\epsilon_0 \sim \mathcal{U}(-0.5, 0.5)$ and $\theta_0 \sim \mathcal{U}(-\pi, \pi)$. Thus, we can firstly initialize $\hat{\mathbf{z}}_0 = \text{E}[\mathbf{z}] = \mathbf{0}$ and $P_0 = diag\{1/12; \pi^2/3\}$ by using the variances of ϵ_0 and θ_0. Then, a recursive update is performed to help realize the dynamic joint estimation. For $n = 1, \ldots, N-1$, we update the prior state estimate $\hat{\mathbf{z}}_n^-$ from the density $p(\mathbf{z}_n|\mathbf{z}_{n-1})$, which is a bivariate normal density. After computing the H_∞ gain K_n, we can get the posterior estimation error covariance matrix P_n^+ and the posterior state estimate $\hat{\mathbf{z}}_n^+$. By utilizing K_n, we can determine whether to trust more in the observations or predicted results by our model. The last state estimate, $\hat{\mathbf{z}}_{N-1}$, will be the final result for joint estimation.

In practical optical transmissions, the noise distributions and covariance matrices are usually unknown. In this case, if we still apply the EKF, which requires all the statistical information of

Optics EXPRESS

the noise terms, there will be a severe degradation on the estimation accuracy. By solving the min-max optimization problem in Eq. (6), the H_∞ filter helps to find the MMSE estimates under extremely noisy conditions, which greatly improves the robustness of the proposed algorithm.

Algorithm 1. H_∞ Filtering for CFO and LPN Tracking

Input: Initialize $\hat{\mathbf{z}}_0 \sim P_{\hat{\mathbf{z}}_0}$ and the estimation error covariance P_0, Q_0;
Compute the partial derivative matrix F_0
Output: State vector estimate $\hat{\mathbf{z}}_{N-1}$
for $n \leftarrow 1$ **to** $N-1$ **do**
  Update prior state estimate: $\hat{\mathbf{z}}_n^- \sim p(\mathbf{z}_n|\mathbf{z}_{n-1})$;
  Calculate the H_∞ gain:
  $K_n = P_n[I - \lambda P_n + H_n^H R_n^{-1} H_n P_n]^{-1} H_n^H R_n^{-1}$;
  Update posterior state estimate:
  $\hat{\mathbf{z}}_n^+ = F_n \hat{\mathbf{z}}_n^- + F_n K_n[y_n - h_n(\hat{z}_n^-, 0)]$;
  Update posterior estimation error covariance:
  $P_n^+ = F_n P_n (I - \lambda P_n + H_n^H R_n^{-1} H_n P_n)^{-1} F_n^H + Q_n$;
end

3.3. Signal detection

Since only the first OFDM symbol is designed as the pilot symbol, to dynamically track the LPN for the entire received signal, we have to know the information about the other transmitted OFDM symbols. Traditional approaches prefer to achieve the phase estimation in the frequency domain. That is, the frequency-domain LPN can be divided into the CPE which leads to the rotation of the constellations and an ICI part which is usually regarded as the AWGN. However, under a high phase noise variance, the effect of ICI cannot be neglected and compensating for the CPE only will cause severe BER performance degradation. Thus in this section, we propose a decision-feedback signal detection approach for dynamic LPN tracking and accurate carrier recovery. This signal detection approach is performed in the time domain since only under this condition, the phase noise can be modelled as the Wiener process and the SSM in Eq. (6) still holds, which ensures the feasibility of dynamic tracking.

The signal detection process can be implemented by the diagram shown in Fig. 1, where N_s is the number of OFDM symbols and k is the symbol index. The detailed steps are summarized as follows:

Step 1: *Joint estimation of CFO and LPN.* Taking the first OFDM symbol as the pilot symbol, we can jointly track the CFO and LPN by utilizing the H_∞ filter mentioned in Section 3.2. Then, since the CFO is a constant, we compensate it for the entire received signal by the mean value of the last l values of the tracked CFO, and denote the estimate as $\hat{\epsilon}$.

Step 2: *Recursive signal detection and phase tracking.* In this recursive update process, we apply the one-dimensional H_∞ filter to track the LPN based on the CFO-compensated signal. Firstly, the H_∞ filter is applied to the first OFDM symbol again to obtain a more accurate phase estimate, $\hat{\boldsymbol{\theta}}_1$. Here $\hat{\boldsymbol{\theta}}_1$ is an N-dimensional vector that is composed of the phase estimation on each subcarrier with an OFDM symbol. Then, to recover the second transmitted symbol, we assume that the phase noise on the second symbol varies slowly so that it can be regarded as a constant phase, and we utilize the average of the last m estimated phases in the first OFDM symbol, $\hat{\phi}_1$, to compensate for and make decision on the second symbol. Next, by utilizing the estimated second transmitted symbol, we can apply the H_∞ filter again to obtain a fine LPN estimate. The final recovered second

Optics EXPRESS

OFDM symbol is the one that is compensated by the newly updated fine phase estimate. A recursive update of these steps is performed symbol by symbol, until we recover all the transmitted OFDM symbols.

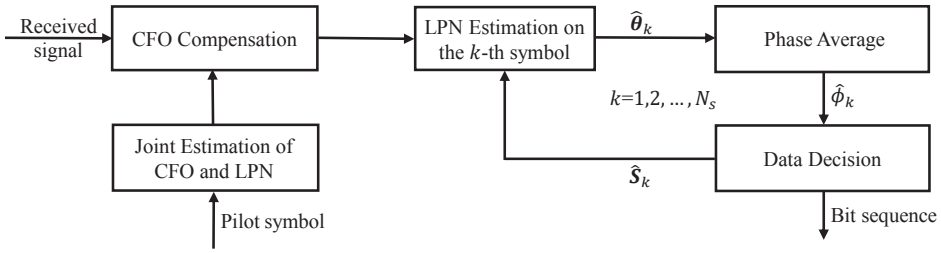

Fig. 1. The diagram of the proposed signal detection scheme.

3.4. Cramér-Rao lower bounds

The CRLB in statistical signal processing theory is a powerful tool to evaluate an unbiased estimator. However, since in the proposed H_∞ filter, the state noise covariance matrix is positive semi-definite (p.s.d), the inverse of Q_n does not exist. To solve this problem, here we consider the CRLBs for the CFO ϵ and the initial phase θ_0 under the assumption that there is no LPN. Then a BCRLB is derived for the LPN $\boldsymbol{\theta}$ given ϵ.

Firstly, under the case when the phase noise variance is equal to 0, the states to be estimated becomes two constants, i.e., ϵ and θ_0. The likelihood function can be expressed as:

$$p\left(\{r_n\}_{n=0}^{N-1}|\epsilon,\theta_0\right) = \left(\frac{1}{\pi\sigma_w^2}\right)^N \exp\left\{-\frac{1}{\sigma_w^2}\sum_{n=0}^{N-1}\left(r_n - s_n e^{j\left[\frac{2\pi\epsilon n}{N}+\theta_0\right]}\right)^2\right\}. \tag{9}$$

Then the Fisher information matrix (FIM) is obtained by calculating

$$\begin{aligned} J &= -\mathrm{E}\begin{bmatrix} \frac{\partial^2 \log p\left(\{r_n\}_{n=0}^{N-1}|\epsilon,\theta_0\right)}{\partial\epsilon^2} & \frac{\partial^2 \log p\left(\{r_n\}_{n=0}^{N-1}|\epsilon,\theta_0\right)}{\partial\epsilon\partial\theta_0} \\ \frac{\partial^2 \log p\left(\{r_n\}_{n=0}^{N-1}|\epsilon,\theta_0\right)}{\partial\theta_0\partial\epsilon} & \frac{\partial^2 \log p\left(\{r_n\}_{n=0}^{N-1}|\epsilon,\theta_0\right)}{\partial\theta_0^2} \end{bmatrix} \\ &= \gamma\begin{bmatrix} \frac{4\pi^2(N-1)(2N-1)}{3N} & 2\pi(N-1) \\ 2\pi(N-1) & 2N \end{bmatrix} \end{aligned} \tag{10}$$

where γ is the SNR. The CRLBs for the CFO ϵ and the initial phase θ_0 are the first and second diagonal element of the matrix J^{-1}, i.e. [13],

$$\begin{aligned} \mathrm{CRLB}_{\hat{\epsilon}} &= \frac{3N}{2\pi^2(N^2-1)\gamma} \\ \mathrm{CRLB}_{\hat{\theta}_0} &= \frac{2N-1}{N(N+1)\gamma} \end{aligned}. \tag{11}$$

Next, we consider the BCRLB for the LPN $\boldsymbol{\theta}$ given ϵ. For simplicity but without loss of generality, the transmitted pilot symbol is assumed containing all ones. The joint probability

Optics EXPRESS

density function of $\mathbf{r}$ and $\boldsymbol{\theta}$ given ϵ can be expressed as [14]

$$p(\mathbf{r},\boldsymbol{\theta}|\epsilon) = p(\theta_0)\prod_{i=1}^{N-1} p(r_i|\theta_i,\epsilon)\prod_{j=1}^{N-1} p(\theta_j|\theta_{j-1}). \tag{12}$$

Decompose $\boldsymbol{\theta}$ as $\boldsymbol{\theta} = [\boldsymbol{\theta}_{N-2}, \theta_{N-1}]^T$, where $\boldsymbol{\theta}_{N-2} = [\theta_0, \theta_1, \ldots, \theta_{N-2}]$ is a $N-1$ dimensional vector, we can express the FIM $J(\boldsymbol{\theta})$ correspondingly as

$$J(\boldsymbol{\theta}) = \begin{bmatrix} A_{N-1} & B_{N-1} \\ B_{N-1}^T & C_{N-1} \end{bmatrix} = \begin{bmatrix} -\mathrm{E}\left[\frac{\partial^2 \log p(\mathbf{r},\boldsymbol{\theta}|\epsilon)}{\partial \boldsymbol{\theta}_{N-2}^2}\right] & -\mathrm{E}\left[\frac{\partial^2 \log p(\mathbf{r},\boldsymbol{\theta}|\epsilon)}{\partial \boldsymbol{\theta}_{N-2}\partial\theta_{N-1}}\right] \\ -\mathrm{E}\left[\frac{\partial^2 \log p(\mathbf{r},\boldsymbol{\theta}|\epsilon)}{\partial\theta_{N-1}\partial \boldsymbol{\theta}_{N-2}}\right] & -\mathrm{E}\left[\frac{\partial^2 \log p(\mathbf{r},\boldsymbol{\theta}|\epsilon)}{\partial\theta_{N-1}^2}\right] \end{bmatrix}. \tag{13}$$

By derivation we have

$$A_{N-1} = \begin{bmatrix} \frac{2}{\sigma_w^2}+\frac{1}{\sigma_v^2} & -\frac{1}{\sigma_v^2} & 0 & \cdots & 0 & 0 \\ -\frac{1}{\sigma_v^2} & \frac{2}{\sigma_w^2}+\frac{2}{\sigma_v^2} & -\frac{1}{\sigma_v^2} & \cdots & 0 & 0 \\ 0 & -\frac{1}{\sigma_v^2} & \frac{2}{\sigma_w^2}+\frac{2}{\sigma_v^2} & \cdots & 0 & 0 \\ \vdots & \vdots & \vdots & \ddots & \vdots & \vdots \\ 0 & 0 & 0 & \cdots & \frac{2}{\sigma_w^2}+\frac{2}{\sigma_v^2} & -\frac{1}{\sigma_v^2} \\ 0 & 0 & 0 & \cdots & -\frac{1}{\sigma_v^2} & \frac{2}{\sigma_w^2}+\frac{2}{\sigma_v^2} \end{bmatrix}, \tag{14}$$

$$B_{N-1} = \left[0, 0, \ldots, 0, -\frac{1}{\sigma_v^2}\right]^T, \tag{15}$$

$$C_{N-1} = \frac{2}{\sigma_w^2}+\frac{1}{\sigma_v^2}. \tag{16}$$

The BCRLBs for $\boldsymbol{\theta}$ can then obtained by finding the diagonals of $J^{-1}(\boldsymbol{\theta})$. In particular, the BCLRB for θ_{N-1} is the last diagonal element of the matrix $J^{-1}(\boldsymbol{\theta})$. However, as N becomes larger, the computational complexity for constructing and calculating the inverse of the FIM becomes higher. To solve this problem, The posterior information submatrices J_{n+1} can be derived by applying a recursion [14]:

$$J_{n+1} = D_n^{22} - D_n^{21}(J_n + D_n^{11})^{-1}D_n^{12} \tag{17}$$

where

$$D_n^{11} = -\mathrm{E}\left[\frac{\partial^2 \log p(\theta_{n+1}|\theta_n)}{\partial\theta_n^2}\right] = \frac{1}{\sigma_v^2}, \tag{18}$$

$$D_n^{12} = -\mathrm{E}\left[\frac{\partial^2 \log p(\theta_{n+1}|\theta_n)}{\partial\theta_{n+1}\partial\theta_n}\right] = -\frac{1}{\sigma_v^2}, \tag{19}$$

$$D_n^{21} = -\mathrm{E}\left[\frac{\partial^2 \log p(\theta_{n+1}|\theta_n)}{\partial\theta_n\partial\theta_{n+1}}\right] = D_n^{12} = -\frac{1}{\sigma_v^2}, \tag{20}$$

$$D_n^{22} = -\mathrm{E}\left[\frac{\partial^2 \log p(\theta_{n+1}|\theta_n)}{\partial\theta_{n+1}^2}\right] - \mathrm{E}\left[\frac{\partial^2 \log p(r_{n+1}|\theta_{n+1})}{\partial\theta_{n+1}^2}\right] = \frac{2}{\sigma_w^2}+\frac{1}{\sigma_v^2}. \tag{21}$$

Thus, the BCRLB of θ_{N-1} is just the inverse of J_{N-1}.

Optics EXPRESS

4. Simulation results and discussion

Simulations are carried out through Matlab and VPI TransmissionMaker, whose setup is shown in Fig. 2. A pseudo-random input data sequence of length $2^{15} - 1$ is modulated onto 16-QAM, then transformed to the time-domain by IDFT of size 256. A 32-sample cyclic prefix is inserted before each OFDM symbol. The sample rate of the arbitrary waveform generator (AWG) is 25 GSa/s. In VPI simulations, the launched power is −2 dBm, and the CLW is set to be 500 kHz. In each span, the length of the fiber loop is 80 km, and the dispersion factor is 16 ps/km/nm. 128 OFDM symbols are transmitted. For the parameters in our algorithm, the initial state vector is determined by utilizing the corresponding expectation, $[0, 0]^T$ and initial estimation covariance matrix P_0 is $diag\{\frac{1}{12}, \frac{\pi^2}{3}\}$. In signal detection, the last 10 CFO estimates are averaged to compensate for the actual CFO through the entire received signal, i.e., $l = 10$ in step 1 of Section 3.3. Similarly, the last 20 LPN estimates are averaged to compensate for the CPE on the next OFDM symbol, i.e. $m = 20$ in step 2 of Section 3.3. To evaluate the estimation performance of the proposed algorithm by using the derived CRLBs in Section 3.4, the pilot symbol is designed to be all ones in Matlab simulations. For GPF, we utilize 500 particles for dynamic tracking and MSE performance comparisons, and 1000 particles for signal detection performance comparisons. The integral part of CFO can be compensated by using our earlier work in [15], which inserts a high-power pilot tone in the middle of the OFDM spectrum, then at the receiver side, the integral part of CFO can be easily obtained by just counting the shifted frequency index of the pilot tone. In the following simulation results, Fig. 3 to Fig. 10 are simulated via Matlab which considers the back to back AWGN channel, Fig. 11 and Fig. 12 are simulated via VPI TransmissionMaker which takes the fiber dispersions and nonlinearities into consideration.

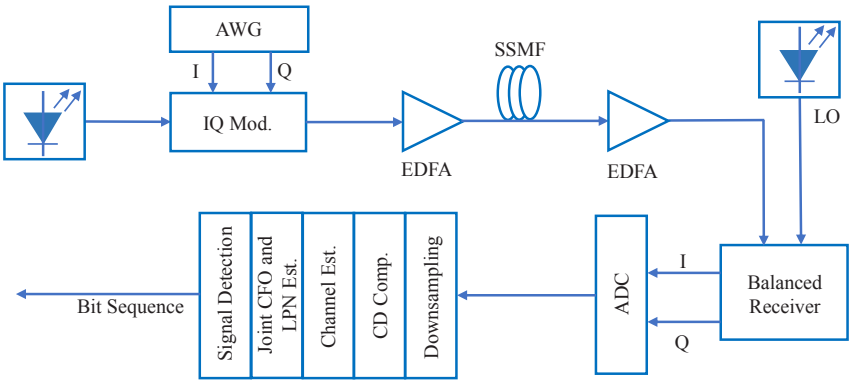

Fig. 2. Simulation Setup (AWG: arbitrary waveform generator, Mod.: modulator, EDFA: Erbium-doped fiber amplifiers, SSMF: standard single mode fiber, LO: local oscillator, ADC: analog to digital converter, Comp.: compensation, Est: estimation).

As what has been illustrated in the optimization problem in Eq. (6), there is a cut-off value of the threshold $1/\lambda$ of H_∞ filter which affects the estimation accuracy and robustness. Figure 3 and Fig. 4 show the MSE of CFO versus λ under 0 kHz and 500 kHz CLW. It can be observed that for any SNR value, the MSE will experience a small fluctuation when λ is moderately low, and then rise sharply when λ reaches the cut-off value. At the same time, as the SNR increases, the cut-off value of λ will gradually increase. The sharp increase of MSE is caused by the fact that it is intractable for the H_∞ filter to find the appropriate optimizer that satisfies a given extremely small threshold under a poor SNR. When the SNR becomes higher, it is possible for the proposed estimator to find the estimate that can achieve lower MSE, which satisfies the given small threshold. However, with the appearance of phase noise, the cut-off point converges to a

Optics EXPRESS

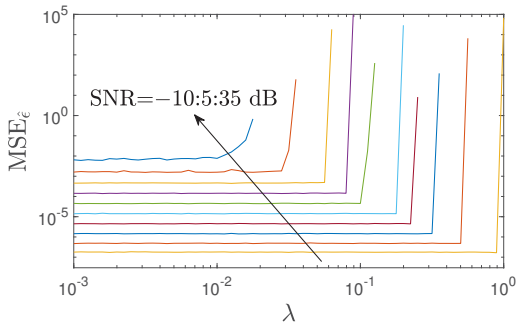

Fig. 3. MSE$_{\hat{\epsilon}}$ of H$_\infty$ filter versus λ under various SNR values, with CLW=0 kHz.

fixed value at a high SNR. There are two main reasons. Firstly, a low SNR means σ_w^2 is large. In this case, a large threshold $1/\lambda$, i.e., λ is small, can ensure the H$_\infty$ filter to tolerate the AWGN. Similarly, when the phase noise appears, although the SNR is increasing, we still need to choose a large threshold to improve the robustness against the phase noise. That is, as σ_w^2 becomes smaller, the effect of LPN dominates. According to Eq. (6), the denominator of the objective function will be mainly affected by Q_n. In this case, the cut-off values of λ at high SNRs will be close to each other. In the following simulations, we choose the cut-off values of λ to implement H$_\infty$ filter according to the results shown in Fig. 3 and Fig. 4, and compare its estimation performance with EKF and GPF.

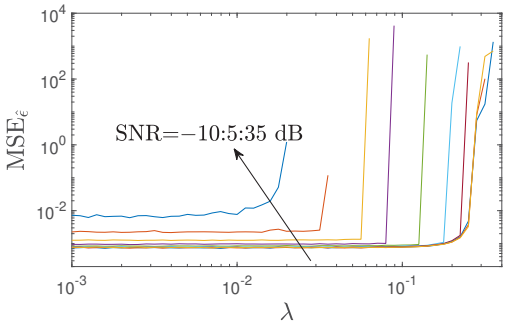

Fig. 4. MSE$_{\hat{\epsilon}}$ of H$_\infty$ filter versus λ under various SNR values, with CLW=500 kHz.

Figure 5 and Fig. 6 show the dynamic tracking performance of H$_\infty$ filter, EKF and GPF with respect to CFO and LPN at 10 dB SNR, respectively. It can be observed from Fig. 5 that the CFO estimates of H$_\infty$ filter and EKF will converge to the steady state within 150 samples which are very close to the actual CFO, while that of the GPF with 500 particles is worse. This is mainly caused by the insufficient number of particles. Figure 6 illustrates that the dynamic phase tracking performance of H$_\infty$ filter is accurate by utilizing the proposed decision-feedback signal detection approach.

As mentioned in Section 3.2, H$_\infty$ filter does not make any assumption about the noise terms. To compare the performance of H$_\infty$ filter, EKF and GPF under the disturbance of the noise term, we introduce a disturbance coefficient ρ. Since these Bayesian filters can only work under the case that the covariance matrices of the noise terms are known, this disturbance coefficient is designed to affect the AWGN noise variance used in the Bayesian filters. That is, the observation noise variance R_n in step 3 and step 5 in Algorithm 1 is enlarged by ρ dB according to the

Optics EXPRESS

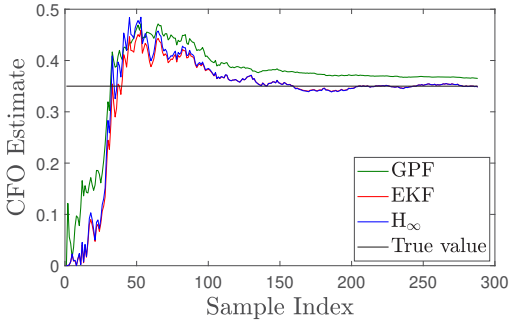

Fig. 5. Dynamic tracking of CFO with SNR= 10 dB, $\epsilon = 0.35$, CLW= 0 kHz.

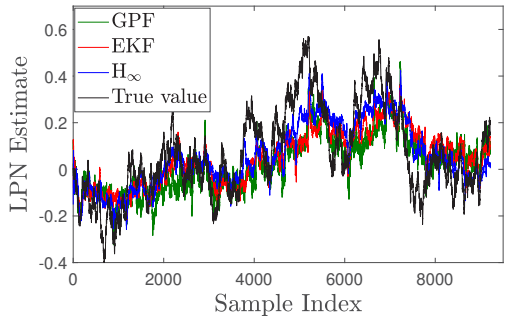

Fig. 6. Dynamic tracking of LPN with SNR= 10 dB, $\epsilon = 0$, CLW= 500 kHz.

following equation:

$$\tilde{R}_n = 10^{\frac{\rho}{10}} R_n. \tag{22}$$

With the appearance of the noise disturbance, Algorithm 1 actually utilizes the disturbed noise variance, i.e., $\tilde{R}_n$ for dynamic state tracking. Figure 7 shows the MSE performance of CFO versus ρ under 5 dB and 15 dB SNR. This figure reveals that under 15 dB SNR, $\text{MSE}_{\hat{\epsilon}}$ values of both H_∞ filter and EKF are stable before ρ reaches up to 10 dB. As ρ exceeds 10 dB, $\text{MSE}_{\hat{\epsilon}}$ of H_∞ filter keeps stable while that of EKF increases obviously. This is because the H_∞ filter focuses on the estimation under the worst cases by solving the min-max optimization problem in Eq. (6). Under 5 dB SNR, even though the MSE of H_∞ filter and EKF both increase, at 20 dB disturbance, the $\text{MSE}_{\hat{\epsilon}}$ of H_∞ is nearly one order lower than that of EKF, which illustrate the excellent robustness of H_∞ filter.

In Fig. 8, we compare the CFO estimation performance of H_∞ with EKF, GPF and conventional Schmidl's approach versus SNR, under the case of no LPN. When there is no disturbance on σ_w^2, $\text{MSE}_{\hat{\epsilon}}$ values of H_∞ filter and EKF can reach the $\text{CRLB}_{\hat{\epsilon}}$, which outperform GPF and Schmidl's algorithms. The main reason is that conventional KF is an optimum linear MMSE estimator, and in this paper, EKF applies a first-order Taylor expansion at the previous estimate, which is very close to the actual nonlinear observation function in Eq. (5). In addition, H_∞ filter becomes EKF when λ approaches 0. Thus, H_∞ filter and EKF show the same performance which converges to the CRLB of CFO. GPF and Schmidl's method cannot reach the CRLB because the estimation accuracy of GPF is highly dependent on the number of particles, and the Schmidl's method takes the correlation between the two identical halves, which is a suboptimal estimator. When there is a disturbance coefficient ρ of 20 dB, there is a significant degradation of the CFO estimation performance of the Bayesian filters. However, the $\text{MSE}_{\hat{\epsilon}}$ increment of H_∞ filter is much lower

Optics EXPRESS

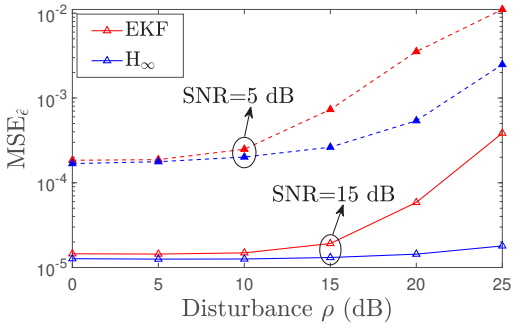

Fig. 7. MSE of CFO versus ρ under SNR= 5 dB and 15 dB, with CLW= 0 kHz.

than that of EKF and GPF and the estimation performance of H_∞ filter can reach the CRLB$_{\hat{\epsilon}}$ quickly at 15 dB SNR. At the MSE of 10^{-4}, the SNR gain of H_∞ filter is nearly 10 dB compared to that of EKF, and 15 dB compared to that of GPF.

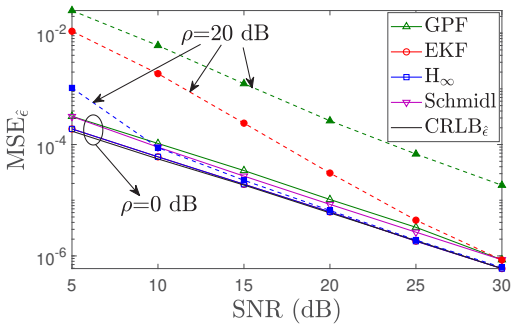

Fig. 8. MSE of CFO versus SNR with ρ = 0 dB and 20 dB, CLW= 0 kHz.

The LPN estimation performance of the proposed H_∞ approach is investigated in Fig. 9 and Fig. 10. Figure 9 shows the effect of the disturbance parameter ρ on MSE$_{\hat{\theta}}$ of H_∞ filter and EKF. This result is consistent with what we have discussed in Fig. 7, which illustrates that the proposed H_∞ filter possesses excellent noise tolerance. In Fig. 10, the MSE of LPN is calculated by using the last phase estimate of the pilot symbol. When the CLW is equal to 0 kHz, the phase noise actually becomes a constant phase whose value is the initial phase θ_0. That is, the BCRLB$_{\hat{\theta}}$ is exactly the CRLB of θ_0 in Eq. (11). It can be observed that the H_∞ filter and EKF can always converge to the BCRLB at even 5 dB SNR, which illustrates their accurate LPN tracking performance. The MSE of GPF gets closer to the BCRLB at a high SNR, but cannot converge to the bound due to the limited particle number.

We then investigate the final signal detection accuracy of the proposed H_∞ approach in terms of BER through VPI TransmissionMaker. Since the Bayesian filters require the information of noise covariance, in our simulations, we mainly consider two cases. The first case is that the AWGN variance σ_w^2 is assumed to be known, i.e., we utilize the following formula to transfer the optical SNR (OSNR) to the electrical SNR [16], and then calculate the actual σ_w^2:

$$\text{OSNR} = \frac{R_s}{2B_{ref}}\text{SNR} \tag{23}$$

where R_s is the symbol rate and B_{ref} is the reference noise bandwidth which is set to be 12.5 GHz in our simulations. Since in real optical fiber transmissions, the AWGN variance is usually

Optics EXPRESS

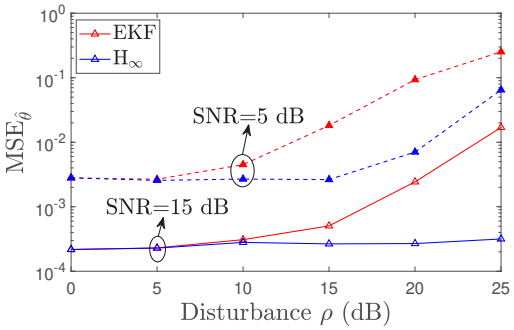

Fig. 9. MSE of LPN versus ρ under SNR= 5 dB and 15 dB, with CLW= 0 kHz.

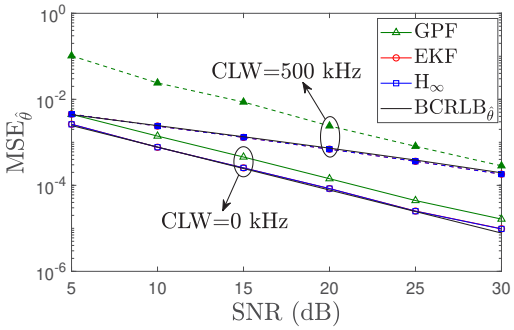

Fig. 10. MSE of LPN versus SNR with $\epsilon = 0$, CLW= 0 kHz and 500 kHz.

unknown, the second case is to estimate σ_w^2 by a straight-forward and simple method, i.e.,

$$\hat{\sigma}_w^2 = \frac{1}{N}\sum_{n=0}^{N-1} |r_n - s_n|^2. \tag{24}$$

Figure 11 presents the BER performance of H_∞, EKF and GPF versus OSNR with 4-QAM and 16-QAM modulation, under the two cases mentioned above, in a back-to-back communication system. Under 16-QAM modulation, it is obvious that the proposed H_∞ filter can achieve the lowest BER even with unknown AWGN variance, whose BER is 1-order lower than that of EKF and 2-order lower than that of GPF. This verifies the excellent robustness and accuracy of the H_∞ filter. When σ_w^2 is known, EKF shows similar BER to the H_∞ filter, whose performance is the best. GPF performs the worst because the randomness of the generated particles may lead to the deviation of the state estimates. Under 4-QAM modulation, the BERs of these three methods are almost the same, since the Euclidean distances of the constellation points are much larger than that of 16-QAM.

Figure 12 investigates BER versus the transmission distance under 16-QAM modulation at 20 dB OSNR, with $\epsilon = 0.35$ and CLW= 500 kHz. Here we utilize the actual AWGN variance σ_w^2 obtained according to Eq. (23) to conduct a clear and complete comparison among these Bayesian filters. The CD is compensated by using the existing algorithm [1]. Here, since the BER performance is highly dependent on the CFO estimation accuracy, we also consider two cases, i.e., compensating by case 1: the estimated CFO $\hat{\epsilon}$ and case 2: the actual CFO ϵ. In Fig. 12, the solid lines represent compensating by $\hat{\epsilon}$, while the dotted lines stand for compensating by ϵ, with 'Comp_ϵ' in the legend. The BER of H_∞ filter under case 1 overlaps with that of case 2, which is increasing as the transmission distance becomes longer. However, EKF and GPF show severe

Optics EXPRESS

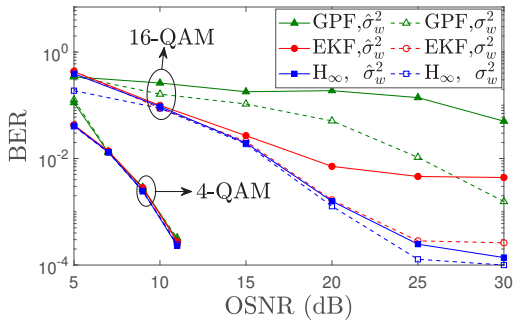

Fig. 11. BER versus OSNR under 4/16-QAM, with ϵ = 0.35 and CLW= 500 kHz.

BER performance degradation in the appearance of residual CD, which means that the obtained CFO estimates are far away from the actual CFO, i.e., their estimation accuracy is sensitive to CD. The comparison in Fig. 12 verifies the robustness of proposed H$_\infty$ filter against CD.

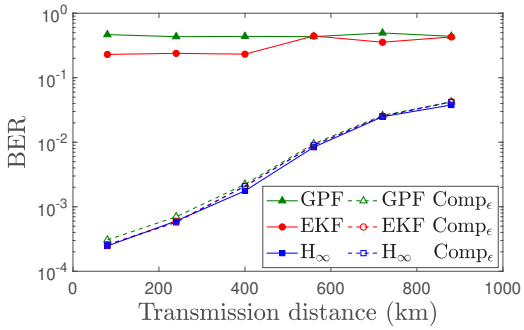

Fig. 12. BER versus transmission distance at 20 dB SNR with CD compensation.

5. Conclusion

A dynamic joint CFO and LPN tracking algorithm was proposed in this paper by utilizing the H$_\infty$ filter for CO-OFDM systems. After the joint estimation, a signal detection method was then derived based on the idea of decision-feedback. Simulation results show that the proposed H$_\infty$ filter algorithm not only has a fast steady-state convergence rate, but also shows excellent tolerance to the external noise disturbance and CD. The MSE of H$_\infty$ filter is nearly 10 dB lower than that of EKF with the appearance of 20 dB noise disturbance, and H$_\infty$ filter can always achieve the best performance of CFO and LPN estimation, which converges to the CRLBs and BCRLB, under uncertain noise statistics. After the 400 km transmission, the final BER of H$_\infty$ filter is still close to 10^{-3} due to its accurate estimation and compensation for the CFO and LPN. Therefore, the superior robustness and accurate joint state estimation make the proposed H$_\infty$ filter-based algorithm be an attractive approach for dynamic carrier recovery in CO-OFDM systems.

Funding. Guangdong Provincial Key Laboratory of Interdisciplinary Research and Application for Data Sciences (2022B1212010006); Guangdong Higher Education Upgrading Plan (2021-2025) (UICR0400001-22, UICR0400009-21); National Natural Science Foundation of China (61971372); Zhuhai Basic and Applied Basic Research Foundation (ZH22017003210016PWC); University Grants Committee (GRF 15200718); UIC Research Grant Project (UICR72021107).

Disclosures. The authors declare no conflicts of interest.

Optics EXPRESS

Data Availability. Data underlying the results presented in this paper are not publicly available at this time but may be obtained from the authors upon reasonable request.

References

1. W. Shieh and I. Djordjevic, *OFDM for Optical Communications* (Academic Press, 2010).
2. M. B. Balogun, O. O. Oyerinde, and F. Takawira, "Efficient constant modulus based carrier frequency offset estimation for CO-OFDM systems," IEEE Photonics J. **9**(5), 1–15 (2017).
3. X. Du, T. Song, Y. Li, M.-W. Wu, and P.-Y. Kam, "An optimum signal detection approach to the joint ML estimation of timing offset, carrier frequency and phase offset for coherent optical OFDM," J. Lightwave Technol. **39**(6), 1629–1644 (2021).
4. M. Zhou, Z. Feng, X. Huang, and Y. Liu, "Maximum a posteriori probability (MAP) joint fine frequency offset and channel estimation for MIMO systems with channels of arbitrary correlation," IEEE Trans. Signal Process. **69**, 4357–4370 (2021).
5. X. Yi, W. Shieh, and Y. Tang, "Phase estimation for coherent optical OFDM," IEEE Photonics Technol. Lett. **19**(12), 919–921 (2007).
6. A. A. Nasir, S. Durrani, and R. A. Kennedy, "Particle filters for joint timing and carrier estimation: Improved resampling guidelines and weighted Bayesian Cramer-Rao Bounds," IEEE Trans. Commun. **60**(5), 1407–1419 (2012).
7. M. Arulampalam, S. Maskell, N. Gordon, and T. Clapp, "A tutorial on particle filters for online nonlinear/non-Gaussian Bayesian tracking," IEEE Trans. Signal Process. **50**(2), 174–188 (2002).
8. P. Priya and D. Sen, "Particle filter based nonlinear data detection in presence of CFO for frequency selective mmwave MIMO-OFDM systems," IEEE Trans. Veh. Technol. **70**(6), 5892–5907 (2021).
9. J. Lim and D. Hong, "Gaussian particle filtering approach for carrier frequency offset estimation in OFDM systems," IEEE Signal Process. Lett. **20**(4), 367–370 (2013).
10. X. Wang, L. Yang, F. Luo, S. Yang, and Y. Du, "Adaptive EKF based estimation method for phase noise in CO-OFDM/OQAM system," IEEE Access **8**, 204931–204940 (2020).
11. L. Li, Y. Feng, W. Zhang, N. Cui, H. Xu, X. Tang, L. Xi, and X. Zhang, "A joint recovery scheme for carrier frequency offset and carrier phase noise using extended Kalman filter," Opt. Fiber Technol. **36**, 438–446 (2017).
12. T. M. Schmidl and D. C. Cox, "Robust frequency and timing synchronization for OFDM," IEEE Trans. Commun. **45**(12), 1613–1621 (1997).
13. X. Du, T. Song, and P.-Y. Kam, "Carrier frequency offset estimation for CO-OFDM: The matched-filter approach," J. Lightwave Technol. **36**(14), 2955–2965 (2018).
14. P. Tichavsky, C. H. Muravchik, and A. Nehorai, "Posterior Cramér-Rao bounds for discrete-time nonlinear filtering," IEEE Transactions on Signal Process **46**(5), 1386–1396 (1998).
15. S. Cao, S. Zhang, C. Yu, and P. Y. Kam, "Full-range pilot-assisted frequency offset estimation for OFDM systems," in *Optical Fiber Communication Conference/National Fiber Optic Engineers Conference 2013*, (Optica Publishing Group, 2013), paper JW2A.53.
16. A. D. Ellis, J. Zhao, and D. Cotter, "Approaching the non-linear Shannon limit," J. Lightwave Technol. **28**(4), 423–433 (2010).